Supplementary figure 1 - relative to Figure 1

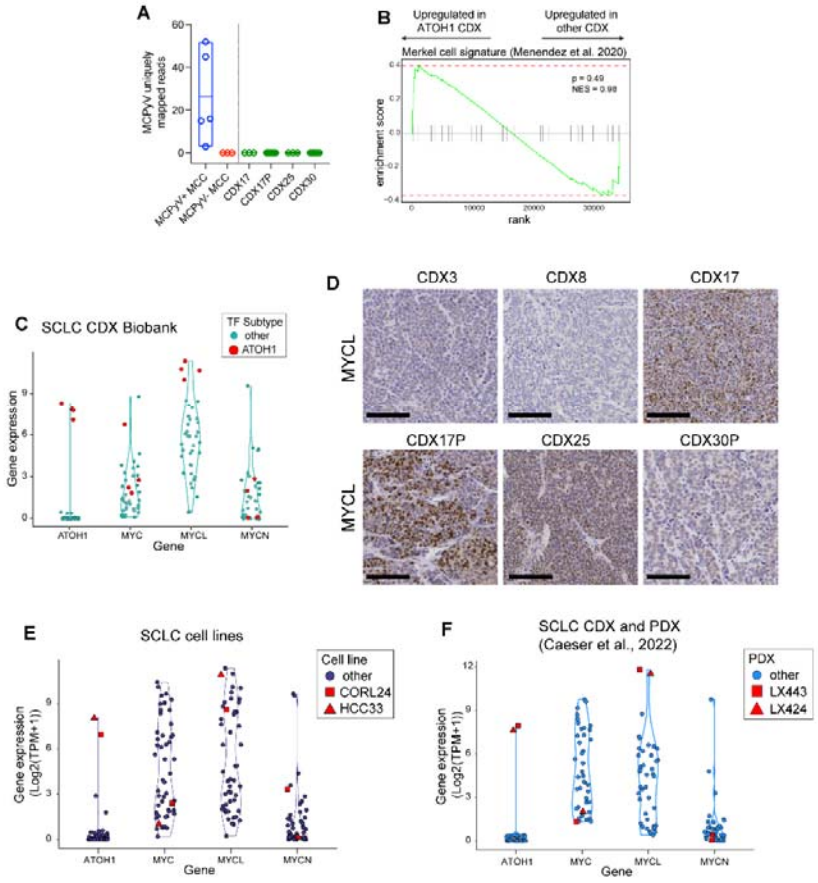

Figure S1. ATOH1 CDX do not have MCC origin and present high expression of MYCL. Relative to Figure 1. (A) Detection of Merkel cell polyoma virus (MCPyV) transcripts in positive and negative control human Merkel cell carcinoma (MCC) samples (PRJNA775071) and ATOH1 CDX. (B) Gene set enrichment analysis (GSEA) for a Merkel cell gene signature from Menendez et al.[35] in ATOH1 CDX (N=4) compared to the whole biobank (N=35). GSEA was performed with Fgsea[103]. (C) Violin plot of expression of indicated *MYC* family genes in the SCLC CDX biobank (N=39). ATOH1 subtype samples and preclinical models highlighted in red. (D) Representative IHC images for MYCL in SCLC-A CDX3, SCLC-N CDX8 and ATOH1 CDX CDX17, 17P, 25 and 30P. (E-F) Violin plot of expression of indicated *MYC* family genes in SCLC cell lines[42] (E) and SCLC PDX[32] (F) from publicly

616 available datasets. ATOH1 subtype preclinical models highlighted in red and
617 annotated by shape as in legend.

Supplementary figure 2 - relative to Figure 3

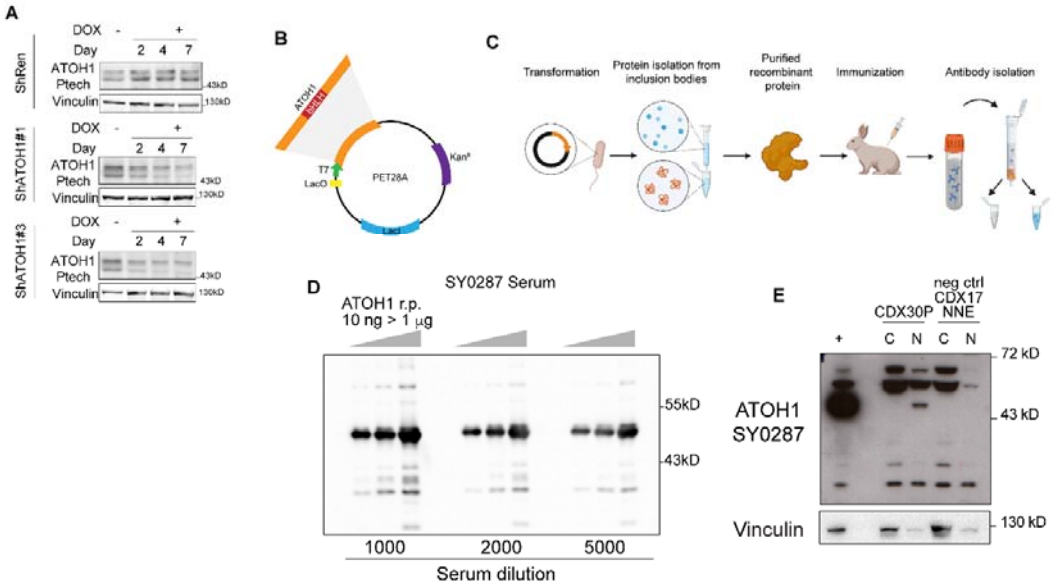

618 **Figure S2. ATOH1 antibody production and validation. Relative to Figure 2.** (A)
619 Western blot showing ATOH1 expression detected by the Ptech antibody over a
620 time-course (0 to 7 days) of ATOH1 knockdown (KD) induction with doxycycline
621 (DOX) in CDX17P. ShRen served as control for ATOH1 KD and Vinculin served as
622 loading control. Western blots are representative of N=2 independent experiments.
623 (B) Schematic of plasmid construct to express ATOH1 recombinant protein in IPTG-
624 inducible PET28A system. (C) Workflow to produce the in-house antibody: ATOH1
625 recombinant protein was purified from bacterial culture and used for immunization of
626 one rabbit. Polyclonal antibodies were isolated from final bleed serum by affinity
627 purification. (D) Test of SY0287 serum before affinity purification against increasing
628 amounts of ATOH1 recombinant protein (10 ng, 100 ng and 1 µg) by western blot.
629 (E) Validation of ATOH1 detection by nuclear (N) and cytoplasmic (C) fractionation of
630 CDX30P (positive control) and CDX17 Non-NE cells (Negative control). Transient
631 ATOH1 overexpression in LentiX 293T cells (indicated as +) served as positive
632 control for detection.

Supplementary figure 3 - relative to Figure 3

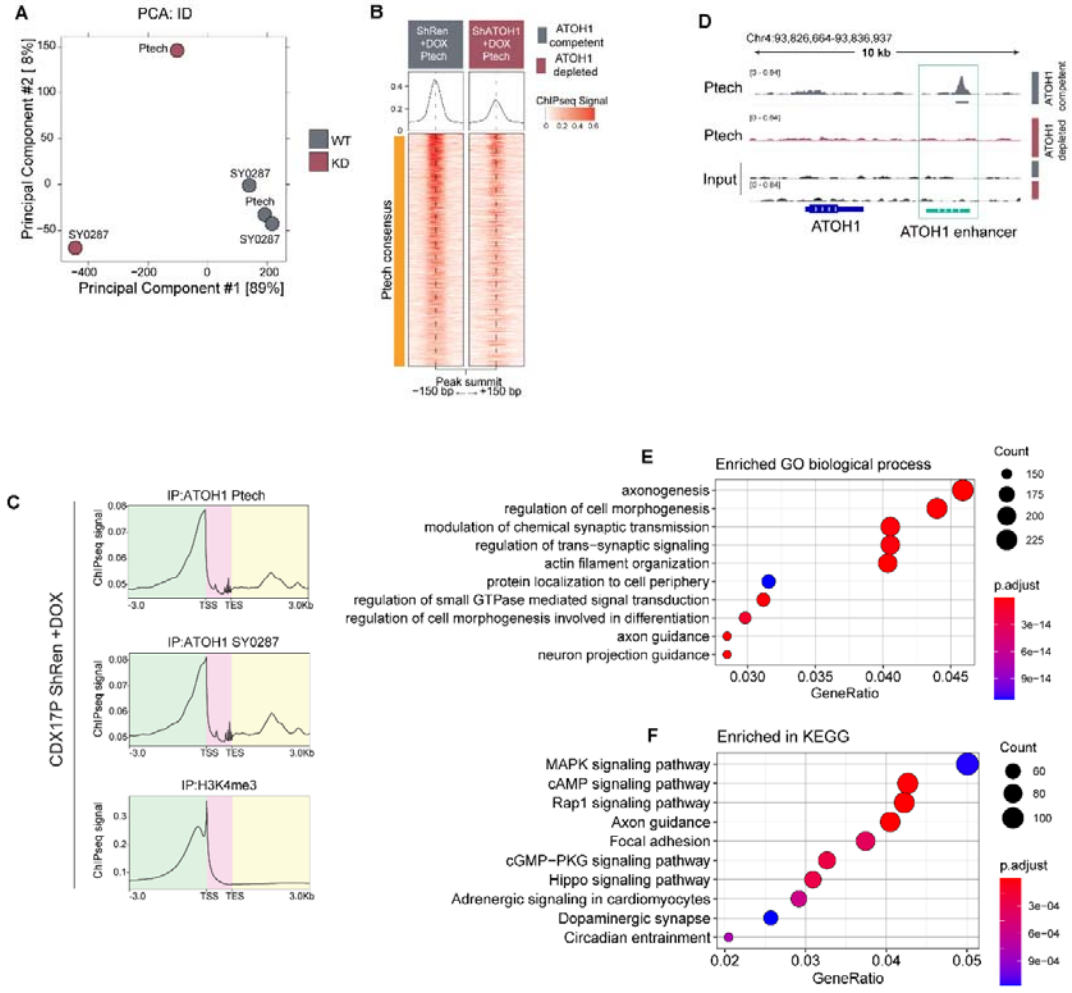

Figure S3. ChIP-Seq samples cluster based on ATOH1 competency and ATOH1 binds to its own enhancer. Relative to Figure 2. (A) Principal component analysis (PCA) of ChIP-Seq samples where ATOH1 competent samples (grey, WT) cluster together and away from ATOH1-depleted samples (red, KD). (B) Heatmap of ChIP-Seq signal for consensus peak sets of Ptech in ATOH1 competent (grey) and depleted (red) CDX17P, generated with the generateEnrichedHeatmap function within profileplyr v1.8.1[100]. (C) Metagene analysis of ATOH1 (detected with Ptech and SY0287) and H3K4me3 ChIP-Seq signal generated with deepTools[104]. Key: green, upstream of gene body; pink, gene body; yellow, downstream of gene body. (D) ATOH1 binding peaks at ATOH1 locus as detected by the Ptech antibody at the ATOH1 downstream enhancer (light green), which are lost upon ATOH1 depletion.

644 The peaks were visualized with the Integrated Genomics Viewer genome browser.
645 (E-F) Gene ontology (GO) biological process (E) and KEGG (F) enrichment analysis
646 of differentially bound ATOH1 peaks identified Figure 3C-i. Analysis was performed
647 with gage[105].

Supplementary figure 4 - relative to Figure 4

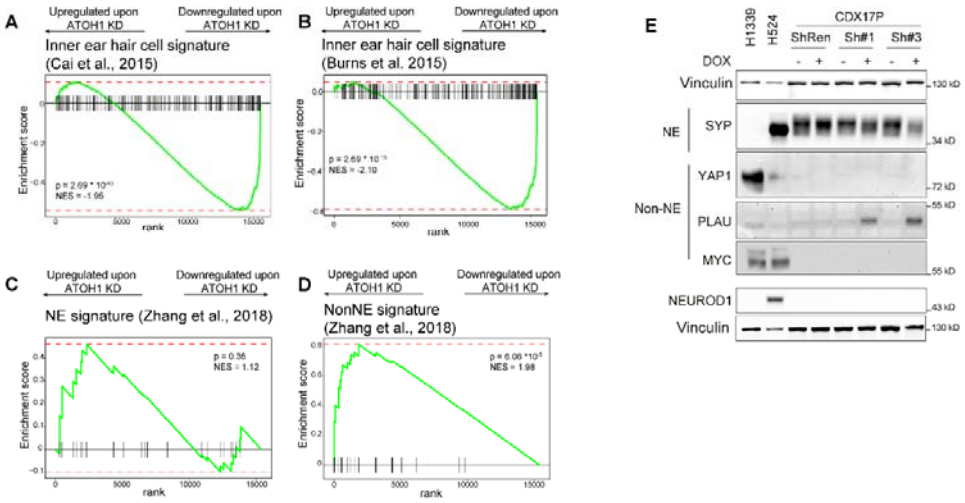

648 **Figure S4. ATOH1 direct targets identified in CDX17P are upregulated in**
649 **ATOH1 CDX. Relative to Figure 4.** (A-B) Gene set enrichment analysis (GSEA) for
650 inner ear hair cell gene signatures obtained from ref[51] (A) and ref[52] (B) upon ATOH1
651 depletion in CDX17P, performed with Fgsea[103]. (C-D) GSEA for NE (C) and Non-NE
652 (D) gene signatures obtained from ref[106]. NES: normalized enrichment score. (E)
653 Western blot expression of NE marker SYP and NonNE markers YAP1, MYC and
654 PLAU after 14 days of ATOH1 knockdown (KD) induction with doxycycline (DOX) in
655 CDX17P. ShRen served as control for ATOH1 KD; H1339 and H524 served as
656 positive controls for expression of YAP1 and MYC; Vinculin served as loading
657 control. Western blots are representative of N=2 independent experiments.

Supplementary figure 5 - relative to Figure 5

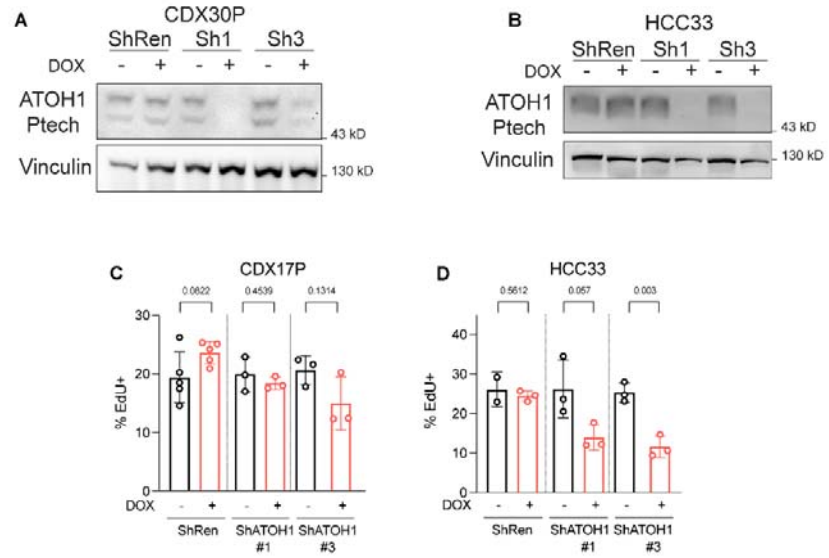

Figure S5. ATOH1 knockdown in CDX17P, CDX30P and HCC33. Relative to Figure 4. (A-B) Representative western blot for ATOH1 in CDX30P (A) and HCC33 (B) cells transduced with ShRenilla (ShRen) and ShATOH1#1 and #3 and treated with DOX for 7 days. (C-D) Bar plot of percentage of cells in S phase, as identified by EdU incorporation, in CDX17P (C) and HCC33 (D) upon ATOH1 depletion. Statistics are reported as two-tailed unpaired *t* test between DOX untreated and treated condition.

Supplementary figure 6 - relative to Figure 6

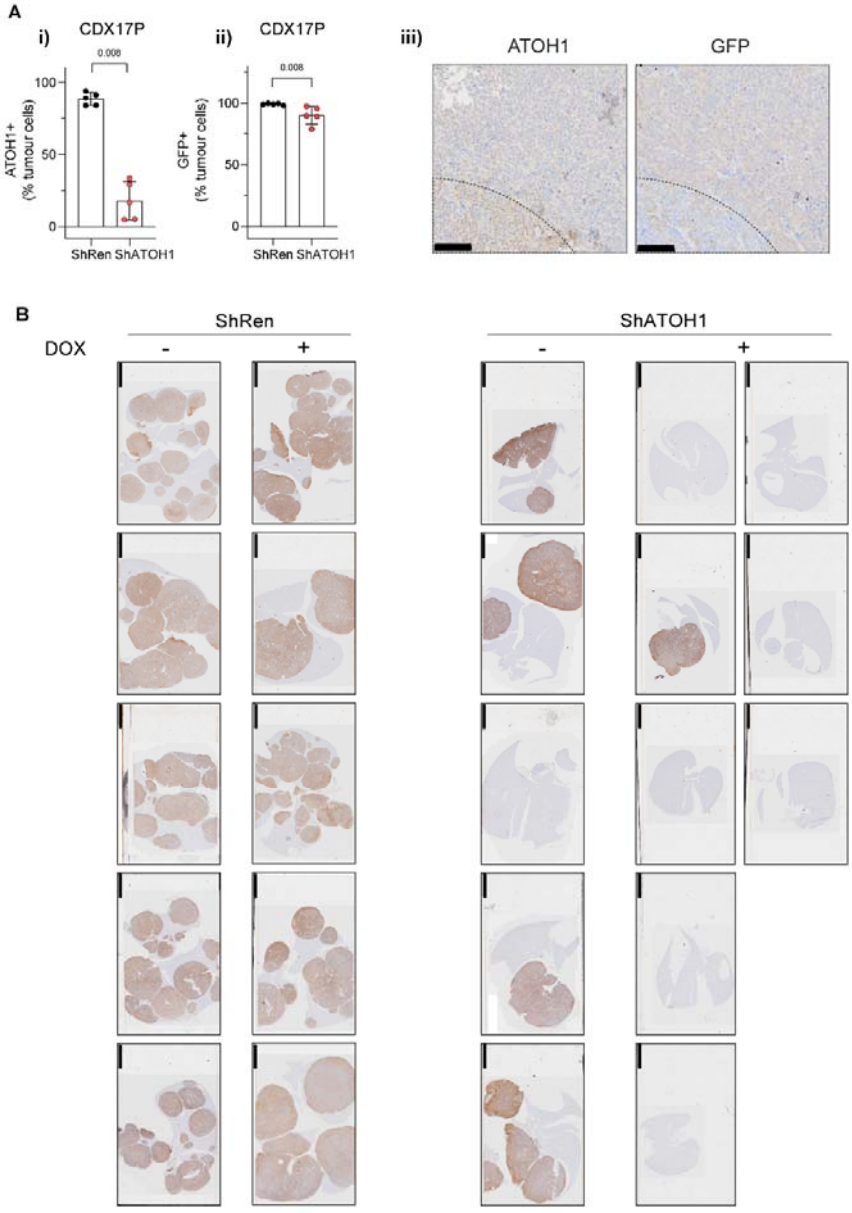

665 **Figure S6. Heterogeneous GFP and ATOH1 expression in ATOH1 KD**
666 **subcutaneous tumours. ATOH1 KD cells exhibit reduced metastatic ability.**
667 **Relative to Figure 6.** (A) Quantification of ATOH1 (A-i) and GFP (A-ii) IHC staining
668 in N=5 subcutaneous tumours from mice implanted with either ShRen or ShATOH1
669 cells and fed DOX-supplemented diet. KD cohort highlighted in red. Statistics
670 reported as per two-tailed unpaired Mann Whitney U test. (A-iii) Representative
671 images of ATOH1 and GFP IHC staining in consecutive sections highlighting parts of

tumours negative for GFP and positive for ATOH1 (dotted lines). Scale bars: 100 µm. (B) IHC staining of human mitochondria in livers from animals that underwent intracardiac implantation of ShRen cells and fed a standard diet (-DOX, N=5) or a DOX-supplemented diet (+ DOX, N=5) or ShATOH1 cells and fed a standard diet (-DOX, N=5) or a DOX-supplemented diet (+DOX, N=8). Only one animal in the ATOH1 KD cohort developed metastasis in the liver. Scale bars: 5 µm.

Acknowledgements

This work was supported through Core Funding to Cancer Research UK (CRUK) Manchester Institute (grant number A27412), Manchester CRUK Centre Award (grant number A25254), the CRUK Lung Cancer Centre of Excellence (grant number A20465), Cancer Research UK Manchester Centre award (CTRQQR-2021\100010), The Christie Charitable Fund, National Cancer Institute R35 CA263816 and U24 CA213274. Patient recruitment was supported by the National Institute for Healthcare Research (NIHR) Manchester Biomedical Research Centre, the NIHR Manchester Clinical research Facility at The Christie Hospital and the CRUK Lung Cancer Centre of Excellence. Sample collection was undertaken through the molecular mechanisms underlying chemotherapy resistance, therapeutic escape, efficacy, and toxicity improving knowledge of treatment resistance in patients with lung cancer or CHEMORES protocol, the TARGET (tumour characterization to guide experimental targeted therapy) study and the CONVERT protocol (concurrent once-daily versus twice-daily radiotherapy: a 2-arm randomised controlled trial of concurrent chemo-radiotherapy comparing twice-daily and once-daily radiotherapy schedules in patients with limited stage small cell lung cancer (SCLC) and good performance status). Dr. Frese, Dr. Simpson and Prof. Dive supervised and devised the study. Dr. Catozzi, Dr. Peiris-Pagès, Dr. Simpson, and Prof. Dive co-wrote the manuscript. Dr. Catozzi, Dr. Peiris-Pagès, Ms. Davies-Williams, Mr. Revill, and Mr. Morgan performed immunohistochemistry analysis, data analysis and interpretation. Dr. Catozzi carried out all experiments on CDX and cell lines, ChIP-Seq, RNA-Seq and western blotting, including data analysis and interpretation. Dr. Catozzi, Dr. Humphrey, Mr. Chen carried out bioinformatics analyses. Dr. Peiris-Pagès designed the *in vivo* metastases studies and analysed the metastatic dissemination of ATOH1